Borehole geophone calibration experiment

Peter Gagliardi, Henry C. Bland[1], and Don C. Lawton

ABSTRACT

Using an Envirovibe vibrator source, calculated geophone orientation azimuths for an 18-level tool were examined in order to determine the effects of stacking and correlation on orientation analysis. Sweeps were 20 s long, and their range was either 10-80 Hz or 10-200 Hz. Using all data points, uncorrelated traces produced standard deviation in the azimuths of 7.90° prior to stacking, and 3.74° after stacking; for correlated traces this was 5.84° prior to stacking and 5.54° after stacking. When the data were split into the separate sweep frequencies, it was found that the higher frequency sweep resulted in less scatter for correlated data, while having little effect on the uncorrelated data. The best statistics were obtained using uncorrelated stacked traces, using shots recorded with the 10-200 Hz sweep, giving a standard deviation of 3.62°. While this is an acceptable amount of scatter, it will still produce errors in offset of more than 6%. It is suggested that the number of shot points, which totalled 11 in this study, should be increased in order to obtain better precision.

INTRODUCTION

As the need to maximise hydrocarbon recovery becomes more prominent, methods such as hydraulic fracturing have become more widespread, and therefore more important to understand; passive seismic monitoring is an important and effective tool employed by oil and gas companies in order to gauge its effectiveness. Monitoring is generally done using measurements taken from 3-component geophones, which are placed into a borehole near the location to be fractured. Unfortunately, when these geophones are placed into a well, their orientation becomes unknown; this can be remedied, however, by performing a calibration survey with known source coordinates. Using these known coordinates, and the amplitude of the first arrivals on each of the components of the geophone, the geophone's orientation can be determined.

However, there are many parameters that can be adjusted for these calibration surveys, and it is not always clear which will have a larger impact on the geophone orientation determination. The aim of this study is to investigate the following questions: what kind of source geometry should be used? In the case of vibroseis, how much impact does the sweep frequency range have? Is it better to use the uncorrelated or correlated data? Is it better to use unstacked shots, and have more data points, or to use stacked shots, and have higher quality data points?

SURVEY PARAMETERS

For this experiment, seismic data was acquired using vibroseis in early 2011; surface conditions are shown in Figure 1. Three lines were recorded (Table 1); Line 1 trended southwest (along the well trajectory), Line 2 trended south and Line 3 trended east (Figure 2). Two types of linear sweeps were examined in this study, 10-80 Hz and 10-200

---

[1] Pinnacle Technologies

Hz; in both cases, the sweep length was 20 seconds long with a 0.25 second cosine taper at the beginning and end of the sweep. Other types of sweeps, as well as a hammer source, were briefly tested in the field but did not produce reliable results; they will not be included in this report. A raw, correlated, shot record showing the horizontal geophone components is shown in Figure 3.

FIG. 1. Picture taken at field site, showing the surface conditions during seismic acquisition. The right side of the picture shows the CREWES EnviroVibe.

Table 1. Summary of acquisition parameters for the survey used in this study.

Line	Number of Shot Locations	Sweeps Used	Minimum Offset from Well (m)	Maximum Offset from Well (m)
1	7	10-80 Hz, 10-200 Hz	183.8	1688.0
2	2	10-80 Hz	1137.1	1499.3
3	2	10-80 Hz, 10-200 Hz	1140.1	1499.5

The well containing the geophones had a maximum deviation of 27.9°, as seen in Figure 4. The tool used was 18 levels, with a receiver spacing of approximately 11.25 m; for the duration of the survey, the top of the tool was at 841 m MD (810 m TVD), and the bottom was at 1032 m MD (982 m TVD). The receivers were not gimballed, so it will be assumed that their vertical components are aligned with the borehole trajectory.

Geometry for Pinnacle VSP Calibration Survey
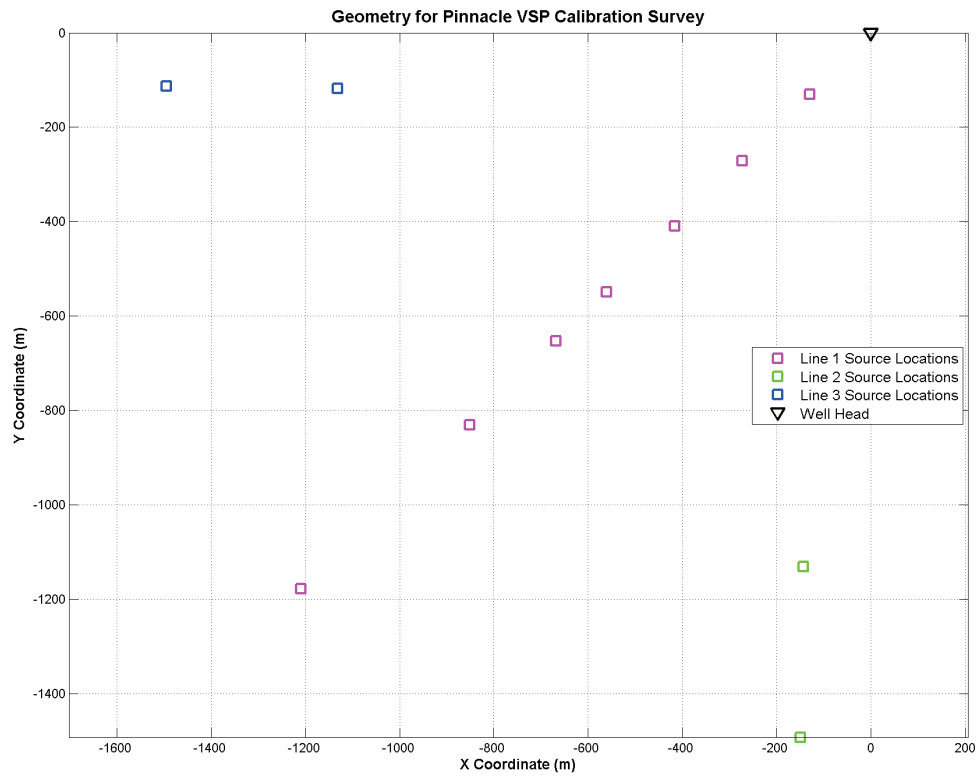
FIG. 2. Surface geometry for the data used in this study; Line 1 is in magenta, Line 2 is in blue and Line 3 is in green. Note that Line 1 roughly follows the deviation path of the well.

Common Shot Gather (Shot 101)
X_{shot} = -130 m, Y_{shot} = -130 m
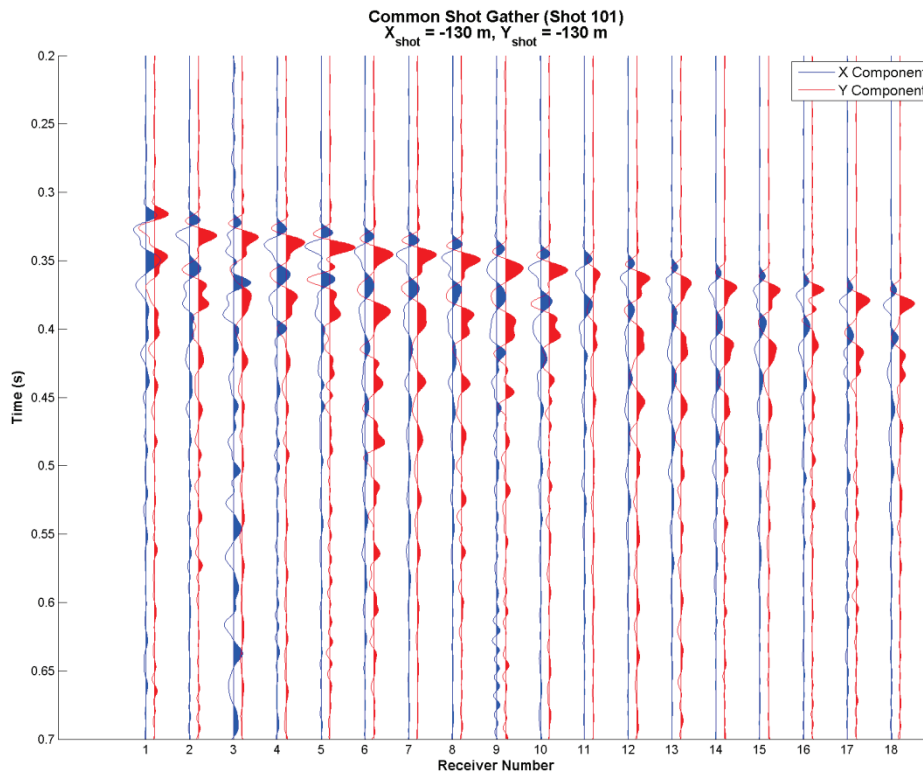
FIG. 3. Example of a correlated common shot gather at shot location 101, prior to stacking. The x-component is shown in blue and the y-component is shown in red.

Pinnacle Well Deviation Survey
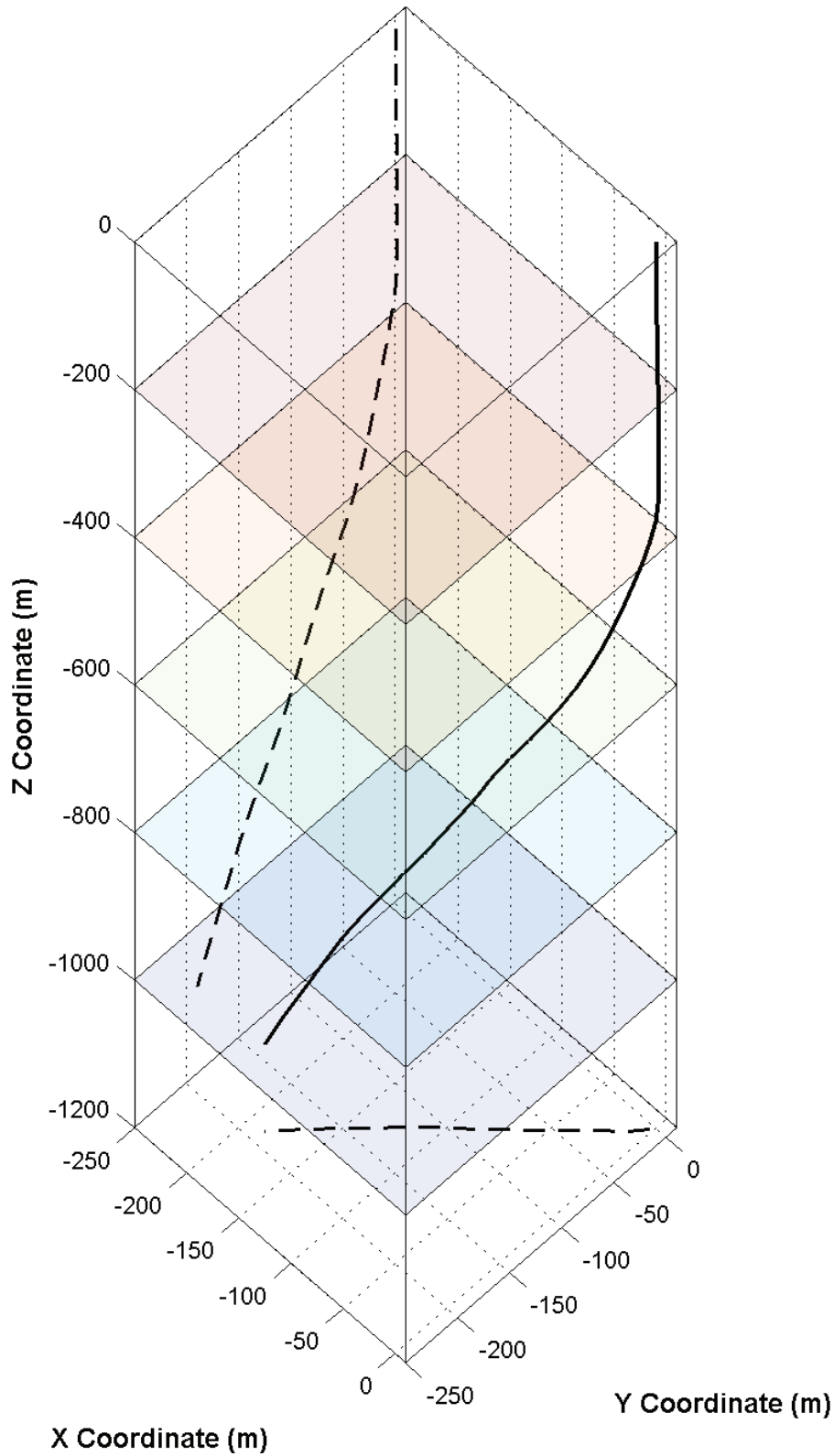
FIG. 4. Deviation survey for well used in this study. The dashed lines are projections of the well onto the y-z and x-y planes. North points in the direction of the positive y-axis.

METHODS

Correlation

In total, four types of data were examined in this study: uncorrelated, correlated, uncorrelated stacked, and correlated stacked. The uncorrelated data has a significantly larger time window that can be analysed for geophone rotation, as the effective wavelet is 20 s long in this case; the wavelet in the correlated case is less than 100 ms long (Figure 3). Correlation was performed using

$$s_c = \sigma \otimes s, \tag{1}$$

where $\otimes$ is a crosscorrelation operator, s is the uncorrelated trace, σ is the vibroseis sweep, and s_c is the correlated data. In the case of correlated stacked traces, the stacking was performed after the correlation. Error may be introduced in the case of uncorrelated stacking due to subtle differences in the vibroseis sweeps, but it was assumed that this error would be relatively unimportant for the purposes of geophone orientation angle calibration. Finally, it should be noted that, for the purposes of stacking, the shot records from the 10-80 Hz sweeps were treated separately from those of the 10-200 Hz sweeps.

Angle calculations

Source-receiver orientation angles were determined analytically, using the equation (DiSiena et al., 1984)

$$\tan 2\theta = \frac{2X \otimes Y}{X \otimes X + Y \otimes Y}, \tag{2}$$

where $\otimes$ is a zero-lag crosscorrelation operator, X and Y are the windowed horizontal component data and θ is the angle between the x-component and source. In the case of correlated data, a window of 100 ms was used, beginning at the first break. In the case of uncorrelated data, the window was from 1.5-18.5 s for the 10-80 Hz sweeps and 1-8 s for the 10-200 Hz sweeps; these windows were determined by visually inspecting the traces. The large windows used for uncorrelated traces may introduce some error, as they encompass reflection events, though the amplitudes observed will still be dominated by first arrivals.

These source-receiver angles must be converted into a more consistent reference frame for each geophone; the equation for a deviated well is given by Gagliardi and Lawton (2011b) as

$$\phi_r = \phi_s' + \theta, \tag{3}$$

where

$$\phi_s' = \arctan(x_s'/y_s'), \tag{4}$$

$$x_s' = \begin{bmatrix} -\sin\phi_w \\ \cos\phi_w \\ 0 \end{bmatrix} \cdot \begin{bmatrix} x_s \\ y_s \\ z_s \end{bmatrix}, \tag{5}$$

and

$$y_s' = \begin{bmatrix} -\cos\theta_w\cos\phi_w \\ -\cos\theta_w\sin\phi_w \\ \sin\theta_w \end{bmatrix} \cdot \begin{bmatrix} x_s \\ y_s \\ z_s \end{bmatrix}. \tag{6}$$

Here, x_s, y_s and z_s are the source coordinates, x'_s and y'_s are pseudo source coordinates, θ_w is the well inclination angle, ϕ_w is the horizontal direction of the well relative to the positive x-axis (i.e. East), θ is defined in Equation 2 and ϕ_r is the geophone azimuth relative to the pseudo y-axis, defined as

$$\hat{y}' = \begin{bmatrix} -\cos\theta_w\cos\phi_w \\ -\cos\theta_w\sin\phi_w \\ \sin\theta_w \end{bmatrix}. \tag{7}$$

More information about this method, including its derivation, can be found in Gagliardi and Lawton (2011b).

RESULTS

Results of angle calculations, plotted against pseudo offset, are shown in Figures 5 – 8. All figures differentiate between line and sweep: Line 1 is shown in magenta, Line 2 in green, Line 3 in blue; shots from the 10-80 Hz sweep are represented as squares and those from the 10-200 Hz sweep are shown as crosses. These data are summarised in Table 2 for all shots, Table 3 for 10-80 Hz sweeps and Table 4 for 10-200 Hz sweeps. Note that one of the horizontal components of receiver 3 wasn't working properly; because of this, it will be ignored for the analysis.

For the unstacked data (Figures 5 and 6), there are noticeable azimuth differences in shots at the same shot location – in some cases this is on the order of 10° or more. Table 2 reveals that the standard deviation of the correlated data, 5.84°, is better than that of the uncorrelated data, 7.90°. The difference between these two datasets is quite significant for certain geophones; the mean orientation of receiver 6 differs by almost 17° between the two datasets! Unfortunately, the angle scatter in both cases is quite high, making it difficult to place confidence in either type of data. For most geophones, there appears to be a large difference in the trend of each line; there are also cases where the different sweep ranges produce markedly different trends. Comparison of Tables 3 and 4 shows that the 10-200 Hz sweep gives a standard deviation about 1.3° better for the correlated unstacked data, and 1.8° better for the correlated stacked data, whereas both types of uncorrelated data seem largely unaffected by the sweep type.

Stacking the data (Figures 7 and 8) shows a couple of interesting effects on the orientation calculations. First, the disparity between the lines seems to be reduced; while there are still differences, they are much less than in the case of the unstacked data. The stacking of the data also significantly improves the scatter of the uncorrelated data, improving it by more than 50%, from 7.90° to 3.74° overall. Interestingly, however, it has little effect on the scatter of the correlated data, only improving it from 5.84° to 5.54°. Comparison of the mean orientation azimuths between the uncorrelated and correlated data after stacking shows much more consistency than prior to stacking, though there are still some differences present.
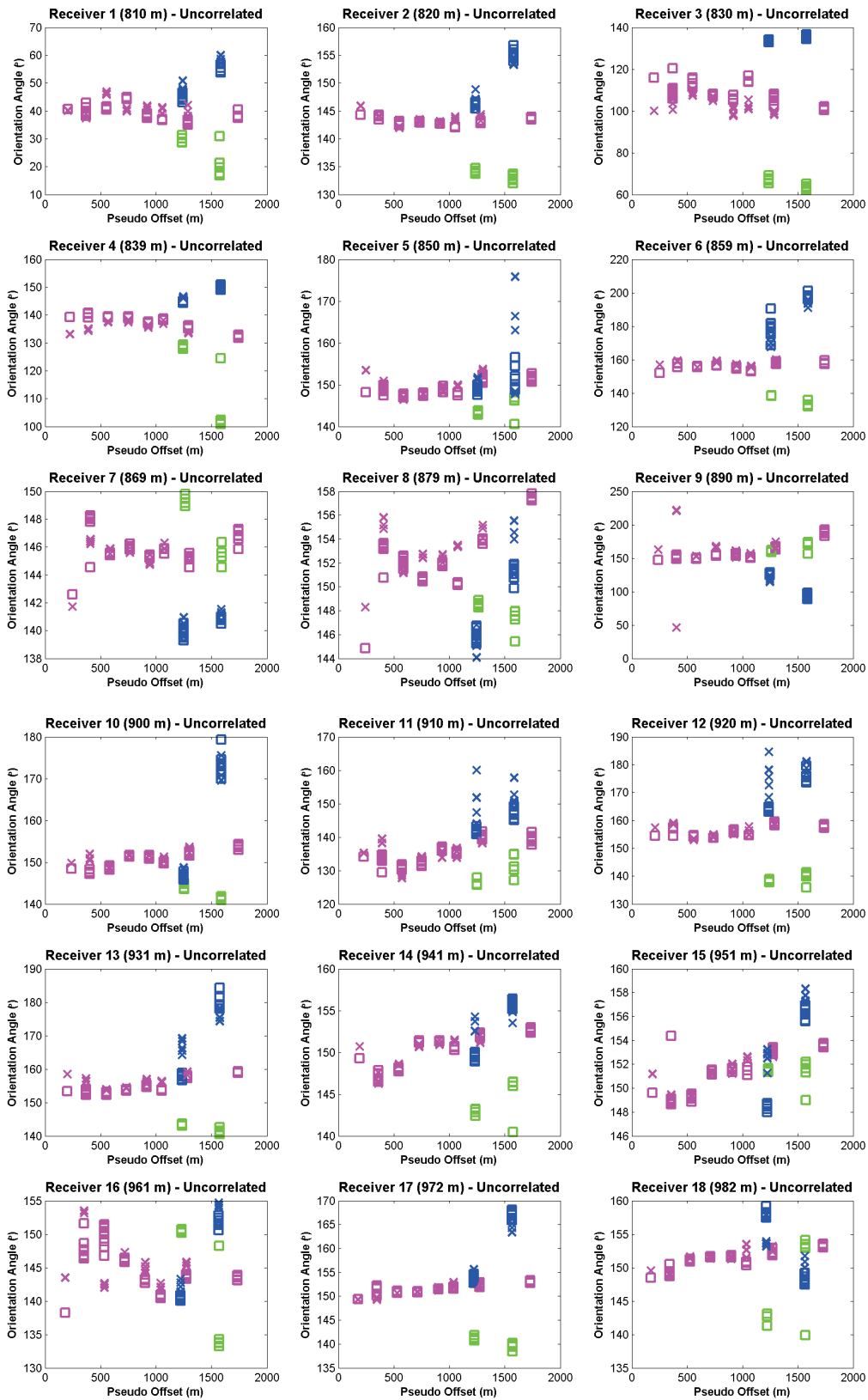
FIG. 5. Geophone orientation azimuth, for uncorrelated unstacked shots, plotted against pseudo offset. Line 1 is shown in magenta, Line 2 in green and Line 3 in blue; squares represent 10-80 Hz shots, crosses represent 10-200 Hz shots.
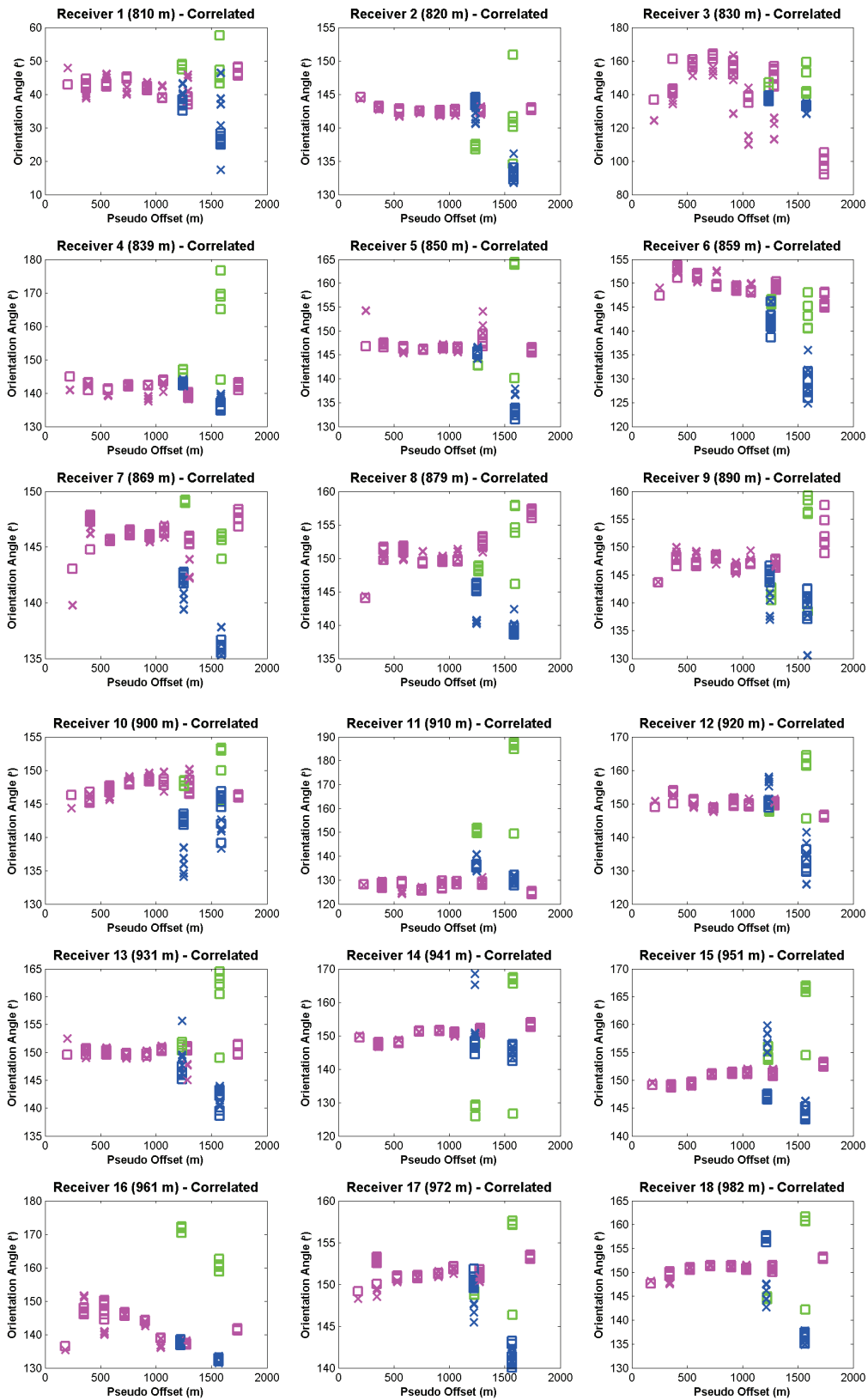
FIG. 6. Geophone orientation azimuth, for correlated unstacked shots, plotted against pseudo offset. Line 1 is shown in magenta, Line 2 in green and Line 3 in blue; squares represent 10-80 Hz shots, crosses represent 10-200 Hz shots.
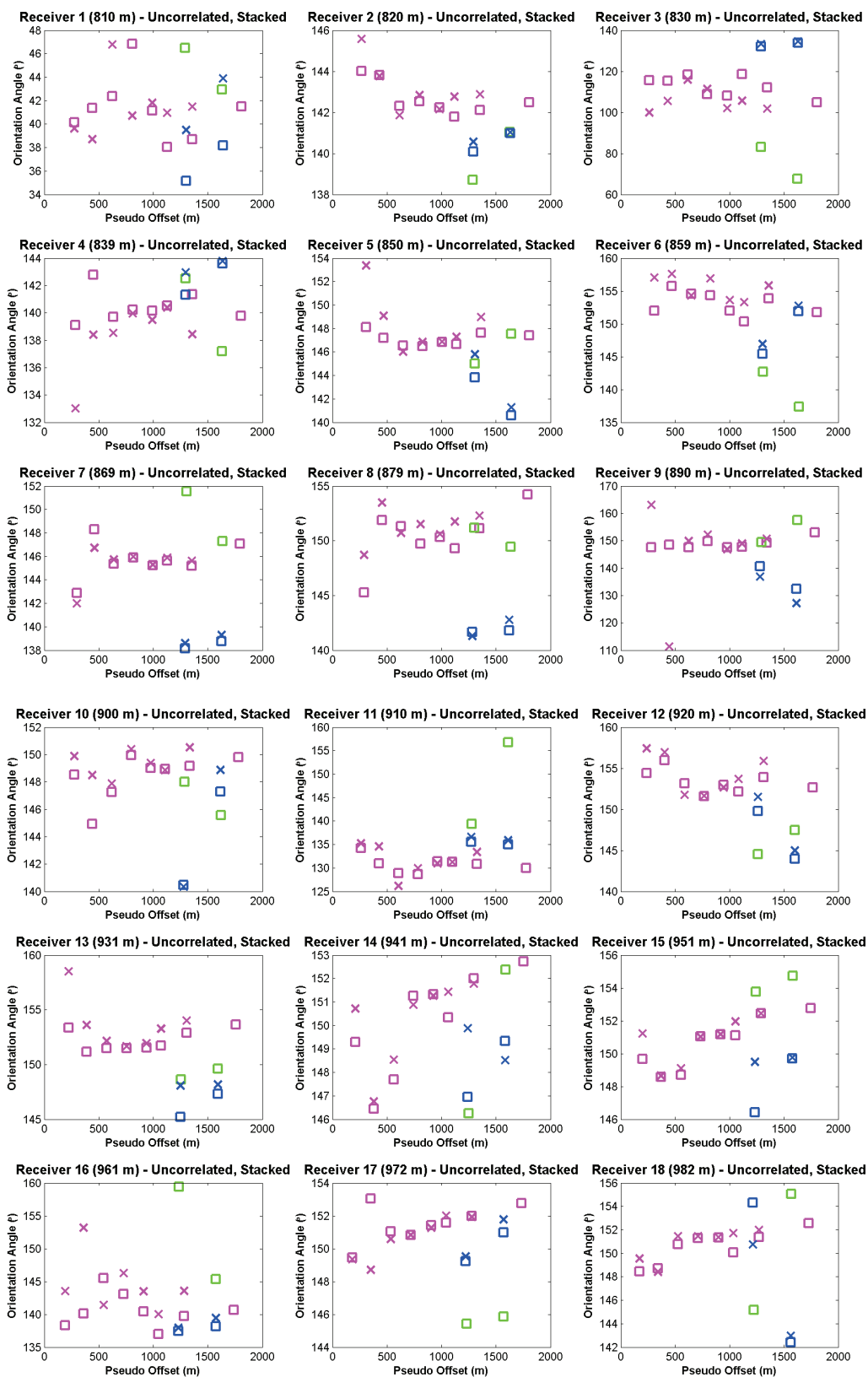
FIG. 7. Geophone orientation azimuth, for uncorrelated stacked shots, plotted against pseudo offset. Line 1 is shown in magenta, Line 2 in green and Line 3 in blue; squares represent 10-80 Hz shots, crosses represent 10-200 Hz shots.
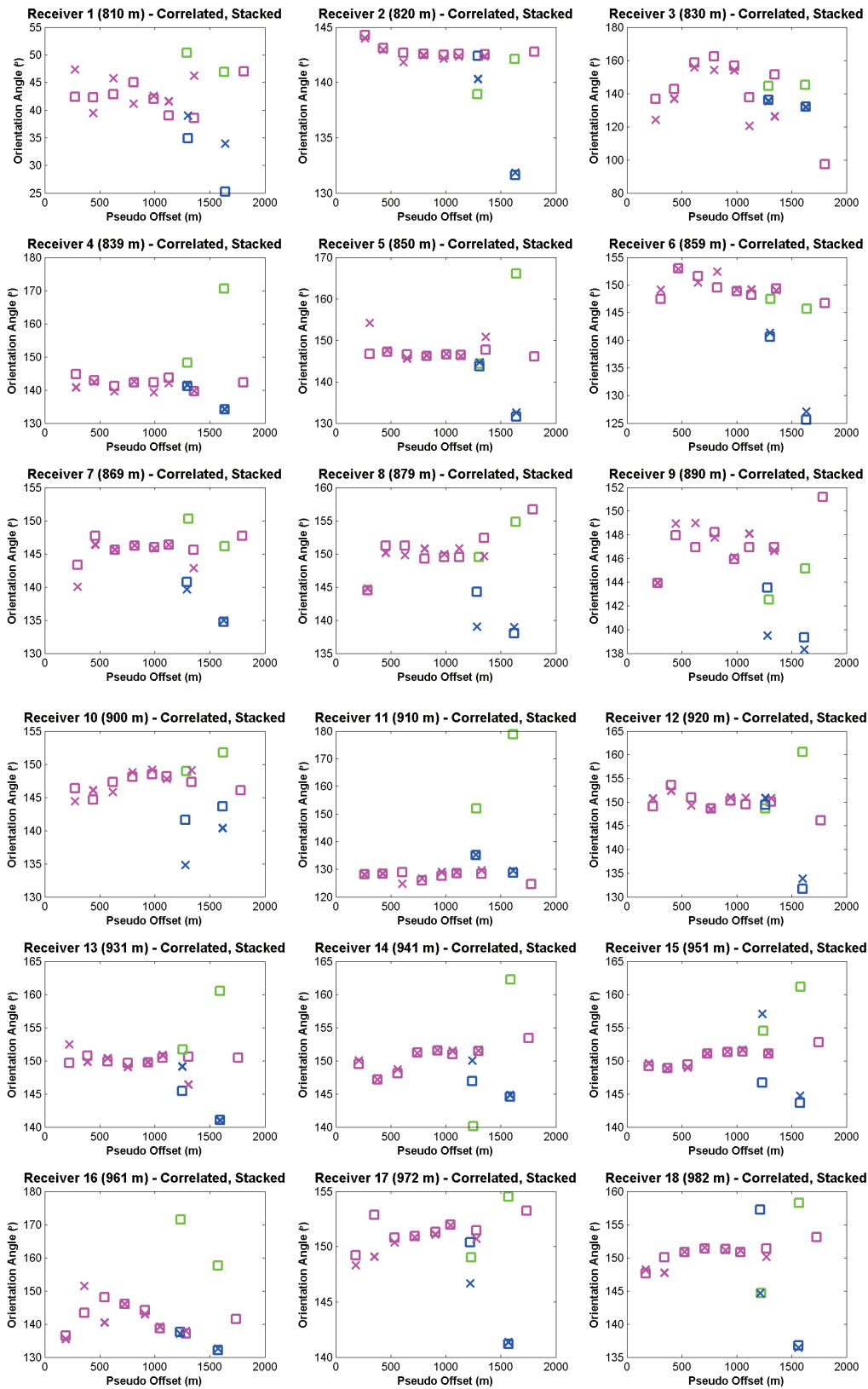
FIG. 8. Geophone orientation azimuth, for correlated stacked shots, plotted against pseudo offset. Line 1 is shown in magenta, Line 2 in green and Line 3 in blue; squares represent 10-80 Hz shots, crosses represent 10-200 Hz shots.

Table 2. Means and standard deviations of geophone orientation azimuth calculations for each receiver; average standard deviation does not include receiver 3. All angles are shown in degrees.

Receiver	Uncorrelated		Correlated		Uncorrelated Stacked		Correlated Stacked	
	Mean	St. Dev.	Mean	St. Dev.	Mean	St. Dev.	Mean	St. Dev.
1	41.4	8.04	40.9	6.05	41.3	2.98	41.6	5.57
2	144.3	5.16	141.3	3.49	142.2	1.50	141.3	3.38
3	110.2	19.26	140.8	16.06	110.9	16.19	140.0	15.47
4	138.0	9.51	142.5	6.28	140.2	2.44	142.6	7.09
5	149.6	4.26	145.7	5.92	146.6	2.64	146.4	6.70
6	162.6	16.33	145.9	7.39	151.9	5.04	146.4	7.38
7	144.5	2.78	144.3	3.73	144.6	3.46	144.2	4.05
8	151.3	3.34	148.7	4.98	149.1	4.00	148.3	4.99
9	147.1	29.37	146.2	4.60	145.6	11.10	145.6	3.41
10	152.1	8.53	146.0	3.53	147.8	2.84	146.1	3.72
11	137.8	7.02	132.8	12.54	133.7	6.16	132.2	12.11
12	159.0	10.28	148.9	6.84	151.9	3.84	148.9	6.04
13	157.8	9.41	149.2	4.17	151.4	2.87	149.5	3.95
14	150.3	3.26	149.4	6.65	149.8	2.06	149.7	4.24
15	151.7	2.54	150.7	4.52	150.7	1.96	150.7	3.79
16	145.5	4.83	143.1	8.93	142.6	5.41	142.7	9.03
17	152.6	6.25	149.9	3.72	150.5	1.98	149.9	3.34
18	151.4	3.44	149.5	6.01	150.1	3.22	149.3	5.30
Average		7.90		5.84		3.74		5.54

Table 3. Standard deviations of geophone orientation azimuth calculations for 10-80 Hz sweeps; averages do not include receiver 3. All angles are in degrees.

Receiver	10 – 80 Hz			
	Uncorrelated	Correlated	Uncorrelated Stacked	Correlated Stacked
1	8.06	6.28	3.40	6.59
2	5.43	3.55	1.48	3.35
3	20.68	16.89	18.60	17.03
4	10.58	7.29	1.76	8.86
5	2.60	6.25	2.12	7.51
6	17.10	7.19	5.53	7.18
7	2.88	3.55	3.75	3.99
8	3.36	4.84	3.96	5.02
9	24.74	4.40	6.18	3.08
10	8.33	2.56	2.69	2.67
11	5.72	14.67	7.70	15.67
12	9.49	6.76	3.84	6.54
13	9.62	4.40	2.53	4.42
14	3.44	7.24	2.36	5.36
15	2.46	4.84	2.38	4.28
16	4.88	9.79	6.14	10.77
17	6.57	3.70	2.45	3.35
18	3.92	6.09	3.59	5.60
Average	7.60	6.08	3.64	6.13

Table 4. Standard deviations of geophone orientation azimuth calculations for 10-200 Hz sweeps; averages do not include receiver 3. All angles are in degrees.

Receiver	10 – 200 Hz			
	Uncorrelated	Correlated	Uncorrelated Stacked	Correlated Stacked
1	6.75	5.60	2.50	4.22
2	4.20	3.37	1.49	3.62
3	15.43	13.74	13.27	13.75
4	6.06	2.05	3.09	2.60
5	6.28	5.18	3.23	5.87
6	14.05	7.96	3.28	8.07
7	2.46	3.88	3.11	4.08
8	3.31	4.89	4.30	4.95
9	37.95	4.82	15.56	3.99
10	8.82	4.95	3.11	4.79
11	8.79	4.02	3.38	2.85
12	10.82	7.13	3.78	5.68
13	8.03	3.51	3.15	3.34
14	2.48	4.99	1.69	2.33
15	2.59	3.78	1.33	3.26
16	4.65	5.50	4.54	5.76
17	5.30	3.44	1.22	3.27
18	1.98	5.34	2.86	4.87
Average	7.91	4.73	3.62	4.33

DISCUSSION

Some key points can be made about the results shown above. First, the effects of stacking the correlated data made little impact on the scatter of the orientation angles, while stacking the uncorrelated data made a significant impact. Additionally, the correlated data had less scatter prior to stacking, while the uncorrelated data had less scatter after stacking. The process of stacking is an effective way of improving signal to noise ratio; similarly, this ratio should be increased by correlation of raw vibroseis data. On the other hand, uncorrelated vibroseis data has a much larger window that can be analysed for the geophone rotation angle; in this case, the window size was 17 s or 7 s, compared to 0.1 s for the correlated data. The result in this experiment shows that, in the context of geophone orientation study, stacking is a more powerful tool for noise removal than correlation is. Of course, this will change for different survey parameters: longer sweeps would improve the effectiveness of correlation, whereas recording more sweeps per shot point would improve the effectiveness of stacking. Thus, for this case, it was most effective to perform the geophone orientation calibration when the traces were uncorrelated and stacked.

Interestingly, the comparison between the different sweep frequencies showed a trend opposite to the effect of stacking. In this case, the correlated seismic was affected more by the sweep, with scatter improving by 1.3° (unstacked) and 1.8° (stacked) when the sweep went to a higher frequency. Scatter in the uncorrelated data actually worsened by 0.3° prior to stacking, and was nearly identical when stacked. It is likely that the smaller window used for the 10-200 Hz sweep is increasing the scatter of the orientation angle; further tests should be performed in order to understand the effects of windowing of the uncorrelated traces.

Finally, it is important to address the issue of acquisition geometry. Other studies by Gagliardi and Lawton (2010, 2011a, 2011b) and Gagliardi et al. (2011) show that farther offsets provide more consistent calibration results; this is due to the increased horizontally propagating energy arriving at the well. In this study the distances of far offsets appear to be comparable; however, the statistics still show quite a high amount of scatter. The best statistics obtained in this study were between 3.62° and 3.74°, depending on the sweep; this amounts to an error of more than 6% in terms of offset. There were only 11 source locations used in this study; given the amount of scatter in orientation azimuth, it would be recommended to add to this number in order to improve statistics calculations. Of course, most factors discussed here will have an economic impact, and their benefit must be assessed in terms of their cost.

CONCLUSIONS

- The standard deviation in geophone orientation azimuth calculations of uncorrelated traces was 7.90° for unstacked data and 3.74° for stacked data.

- The standard deviation in geophone orientation azimuth calculations of correlated traces was 5.84° for unstacked data and 5.54° for stacked data.

- Comparison of sweep frequencies showed that the 10-200 Hz sweep produced better orientation azimuth calculations than the 10-80 Hz sweep for correlated data; however, sweep frequency had little effect on the uncorrelated data.

- It was determined that, in this experiment, uncorrelated, stacked data produced results with the least amount of scatter in geophone orientation azimuth.

- The best results showed a standard deviation of 3.62°; this is an acceptable amount of scatter, though it will still produce noticeable error. Increasing the number of shot points, especially at farther offsets, should be considered in order to improve this number.

FUTURE WORK

Further examination of sweep lengths and frequencies, as well as comparison with dynamite sources, would help to determine the optimal survey parameters for a geophone orientation calibration. Additional work could be done to determine the optimal number of shot locations. Effects of geology should also be investigated, such as that of dipping beds, in order to understand the differences in the three lines used in this study. Finally, windowing tests should be performed on the uncorrelated data in order to determine the sensitivity of the calculations to this parameter.

ACKNOWLEDGEMENTS

REFERENCES

DiSiena, J. P., Gaiser, J. E. and Corrigan, D., 1984, Three-component vertical seismic profiles; orientation of horizontal components for shear wave analysis, in Toksoz, M. N. and Stewart, R. R., eds., Vertical seismic profiling, Part B Advanced concepts: , 189-204.

Gagliardi, P. and Lawton, D. C., 2011, 3D borehole geophone orientation study, central Alberta: CREWES Research Report, **23** (this report)

Gagliardi, P. and Lawton, D. C., 2011, Geophone azimuth consistency from calibrated vertical seismic profile data: CREWES Research Report, **23** (this report)

Gagliardi, P. and Lawton, D. C., 2010, Borehole geophone repeatability experiment: CREWES Research Report, **22,** 22.1-22.23.

Gagliardi, P., Innanen, K. A. H. and Lawton, D. C., 2011, Effects of noise on geophone orientation azimuth determination: CREWES Research Report, **23** (this report)